energies

MDPI

Article

Application of Far-Gather Seismic Attributes in Suppressing the Interference of Coal Beds in Reservoir Prediction

Yunxin Mao [1], Chunjing Yan [2], Ruoyu Zhang [1], Yangsen Li [1], Min Lou [1], Luxing Dou [2], Xinrui Zhou [2] and Xixin Wang [2,*]

[1] Shanghai Branch of CNOOC China Limited, Changning District, Shanghai 200050, China; maoyx@cnooc.com.cn (Y.M.); zhangry10@cnooc.com.cn (R.Z.); liys9@cnooc.com.cn (Y.L.); loumin2@cnooc.com.cn (M.L.)

[2] School of Geosciences, Yangtze University, Wuhan 430100, China; 2021710351@yangtzeu.edu.cn (C.Y.); luxingdou@yangtzeu.edu.cn (L.D.); 2021710354@yangtzeu.edu.cn (X.Z.)

* Correspondence: wangxixin86@yangtzeu.edu.cn

Abstract: The sandstone reservoir of the Pinghu Formation in the Xihu Depression, East China Sea is characterized by great depth, small thickness, radical facies change and a widespread coal bed. It is difficult to describe the reservoir accurately using conventional reservoir prediction methods. In order to analyze the influence of coal-bearing strata on the prediction of the mid-low thickness sandstone reservoir, the seismic response of different sandstone–coal stratigraphic assemblages was simulated by seismic forward modeling. The modeling result indicates that the post-stack seismic response is dominated by coal bed, whereas the response of sandstone can hardly be recognized. In contrast, the difference between the pre-stack AVO (amplitude versus offset) response characteristics of coal seams and gas-bearing sandstones has been clarified based on the statistics pertaining to AVO characteristics of drilled wells. Therefore, we propose a method to reduce the interference of coal beds in sandstone reservoir prediction using far-gather seismic information. This method has significantly improved the accuracy of reservoir prediction and sand description in sand–coal coupled environments and has been applied successfully in the exploration of coal-rich strata in the Pingbei slope belt, Xihu Depression.

Keywords: coal strata; seismic response; pre-stack AVO forward; dominant far-offset; reservoir prediction

Citation: Mao, Y.; Yan, C.; Zhang, R.; Li, Y.; Lou, M.; Dou, L.; Zhou, X.; Wang, X. Application of Far-Gather Seismic Attributes in Suppressing the Interference of Coal Beds in Reservoir Prediction. *Energies* **2022**, *15*, 2206. https://doi.org/10.3390/en15062206

Academic Editor: Reza Rezaee

Received: 20 February 2022
Accepted: 14 March 2022
Published: 17 March 2022

1. Introduction

The western slope zone of the Xihu Depression, which has a high success rate for hydrocarbon drilling and considerable hydrocarbon resources, is one of the most favorable hydrocarbon enrichment areas in the East China Sea [1–3]. However, coal-bearing strata are widespread in the study area. It is difficult to accurately predict the distribution of reservoirs because coal seams and gas reservoirs have many similarities in post-stack seismic analyses, such as low velocity, low P-impedance and bright spots. Consequently, an effective method of suppressing coal bed interference would be of great benefit to reservoir prediction and sustained hydrocarbon production in the East China Sea. Many previous studies on the distribution, formation mechanism and prediction methods of coal beds have been conducted [4,5]. Diessel [6] studied the development of coal seams based on sequence stratigraphy theory for the first time and proposed that coal seams are mainly developed from late Lowstand System Tracts to early Transgressive System Tracts, and from late Transgressive System Tracts to early Highstand System Tracts. The seismic response of reservoirs adjacent to coal seams is difficult to identify because the oil and gas target layers can be affected by the strong amplitude of the coal seam. Many methods focused on strong-amplitude suppression of coal seams have been proposed [7–9]. Based on the amplitude characteristics of weak seismic signals in thick and thin layers, Han and Zhang [10], and Ping [11,12] analyzed the spectrum characteristics of seismic weak

signals, including how they are influenced by noise. The Wigner–Ville distribution, which is a time–frequency analysis method, is used along with multi-wavelet decompression–reconstruction technology to identify coal beds and to exclude the interference of coal beds. A nail-type wavelet and compressed sensing technology were used to remove the strong shield interference so that the seismic response of the target layer was highlighted, and the ability to predict sandstone reservoirs was improved [13]. Zhang et al. [14] successfully suppressed the subwave parametrization using subwave spectral shaping of the raw seismic data; by implementing this technique in combination with compressed sensing processing, they were also able to achieve rejection of strongly shielded signals. Gu et al. [15] adopted a new high-resolution inversion technology that makes full use of lateral seismic waveform space change information instead of a traditional variogram, and they achieved high-precision thin reservoir prediction even under a strong shielding effect. However, it is difficult to describe thin coal seams by seismic data alone due to the small thickness and random distribution of coal. Seismic forward modeling is a valid method of identifying the seismic response of coal seams [16–18]. Moreover, an approach based on AVO characteristics has advantages in detecting special lithology and fluids. Pre-stack seismic analysis highlights special lithological information better than post-stack seismic analysis [18–25]. Therefore, it is also necessary to investigate the reflection mechanism of coal seams so that the influence of coal seams on reservoir prediction can be reduced.

Based on petrophysical characteristics of the coal seams in the study area, we investigate the differences in elastic parameters between coal seams and sandstone or mudstone and identify the distinguishing parameters that can indicate coal seams. The seismic response of different sand–coal stratigraphic assemblages is simulated by seismic forward modeling. The modeling result indicates that the post-stack seismic response is dominated by coal bed, whereas the response of sandstone can hardly be recognized. In contrast, the difference between the pre-stack AVO response characteristics of coal seams and gas-bearing sandstones has been clarified based on the statistics pertaining to AVO characteristics of drilled wells. Therefore, we propose a method to reduce the interference of coal beds in sandstone reservoir prediction using far-gather seismic information. This method has significantly improved the accuracy of reservoir prediction and sand description in sand–coal coupled environments and has been applied successfully in the exploration of coal-rich strata in the Pingbei slope belt, Xihu Depression.

2. Geological Setting

The East China Sea Shelf Basin (ECSSB) is a Meso-Cenozoic superimposed basin lying in the east margin of the Eurasian continental plate. The basin is bounded by the Chinese mainland to the west and by the Okinawa Trough to the east. The Xihu Depression, which is located in the eastern part of the ECSSB and is predominantly NNE-striking, is the largest depression of the ECSSB [26,27]. The Xihu depression can be divided into three tectonic elements: The Western Slope Belt, the Central Inversional Structural Belt and the Eastern Half-graben Belt. The area studied in this paper, the Pingbei slope belt, is located in the north of the Western Slope Belt (Figure 1). The Xihu Depression has been developed since the end of the Mesozoic and is predominantly filled with Cenozoic clastic sediments. The basin's evolution is composed of two phases: the early syn-rift phase was due to extension from the end of the Cretaceous to the Paleocene, and the following post-rift phase was due to thermal subsidence from the Eocene to the Oligocene [28–30].

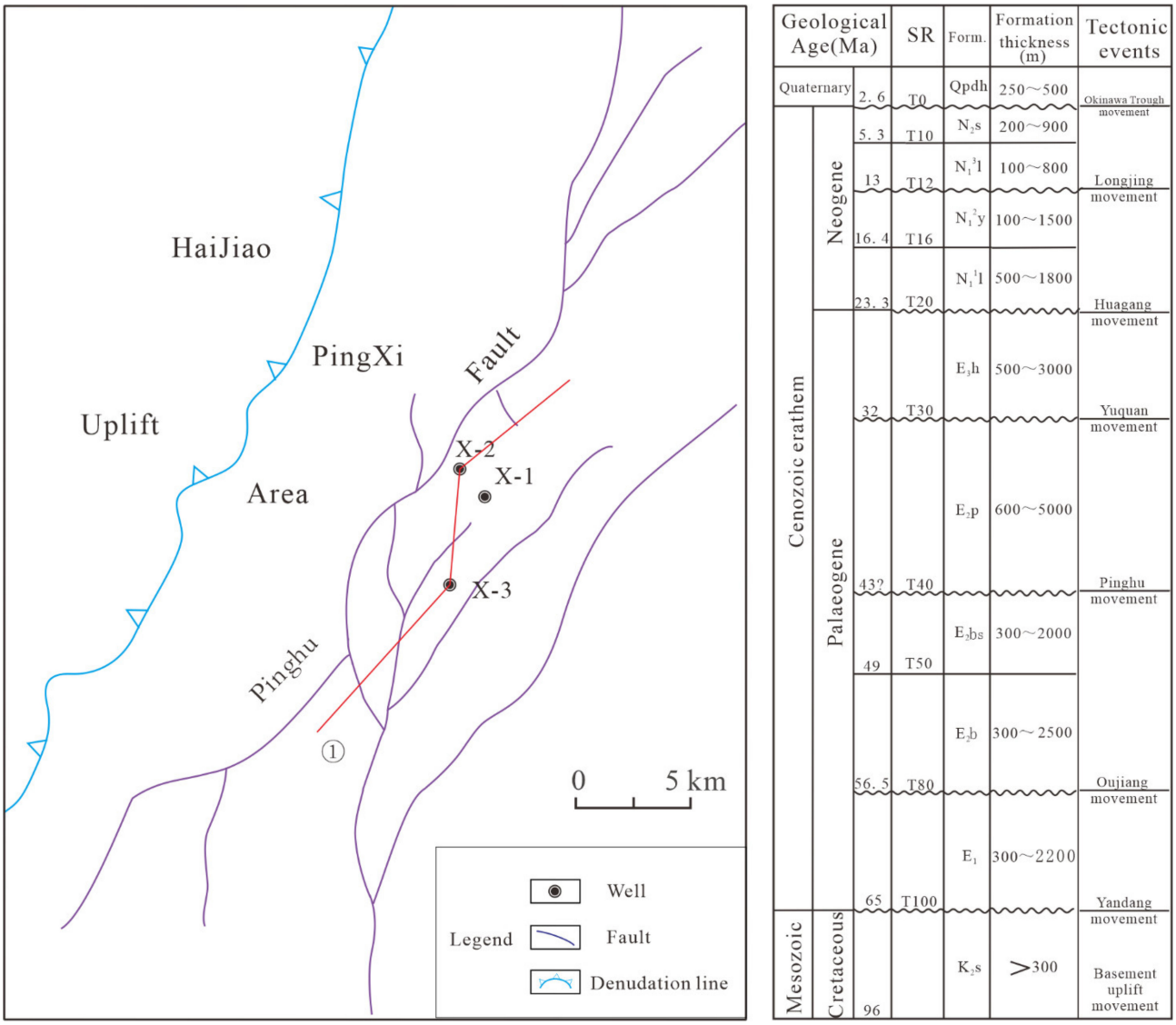

Figure 1. Primary geological structures and the regional stratigraphy in the study area. Locations of wells and seismic profiles in Figure 9 are indicated.

The Pinghu Formation was deposited during the Eocene and comprises interbedded mudstone, siltstone and thin coal beds. Comprehensive analysis of data from the Pinghu Formation in the study area, including seismic phase, drilling core, and logging data, suggests that the coal seam developed mainly in the sedimentary environment of the tidally influenced deltaic plain, the tidally influenced deltaic foreshore divergent interfluve, the supratidal zone and the braided river deltaic foreshore divergent interfluve. The coal beds are interbedded with sandstone and mudstone in the Pinghu Formation. The interbedded layers have small thicknesses ranging from 0.5 to 2 m. The coal beds are difficult to recognize throughout the study area because their lateral change is radical (Figure 2).

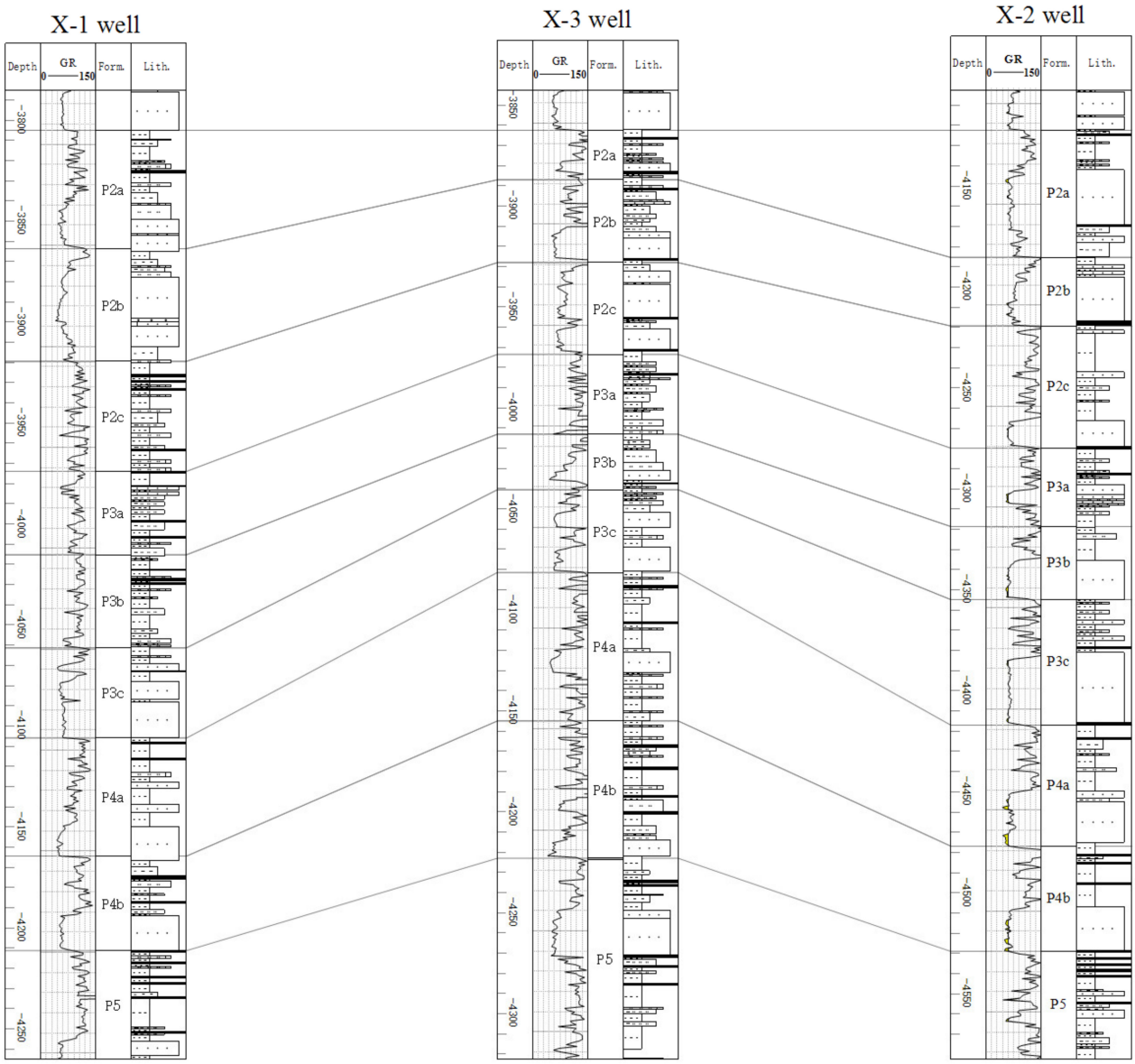

Figure 2. Litho-stratigraphic units of the Pinghu Formation in the Xihu Depression. For locations of the wells, see Figure 1.

3. Data and Methods

We investigate the distribution and reflective characteristics of coal-bearing strata, sandstone and mudstone by means of petrophysics, post-stack forward modeling and pre-stack wave equation forward modeling. First, the petrophysical properties of different lithology assemblages are clarified based on statistics. Second, a series of post-stack and pre-stack forward models are designed and simulated according to the petrophysical characteristics. The modeling result indicates that post-stack seismic analysis demonstrates ambiguity due to the interference of coal seams with the amplitude, frequency and phase of sandstone. Finally, we suppress the interference of coal seams using far-offset partial stacked seismic analysis, taking advantage of the fact that the energy of coal seams decreases as the offset angle increases.

3.1. Analysis of Petrophysical Characteristics

The target layers in the study area are generally buried deeper than 4000 m. The distribution characteristics of P-impedance differ based on lithology (Figure 3), with sandstone P-impedance being the largest, mudstone P-impedance the second largest, and coal seam

P-impedance the smallest. The sandstone P-impedance decreases when the sandstone contains gas, such that the sandstone and mudstone P-impedance are indistinguishable. Hence, only coal seam lithology can be effectively distinguished by P-impedance. In contrast, statistics concerning the ratio of compressional and shear wave velocity (hereafter referred to as Vp/Vs) of different lithologies show that Vp/Vs can effectively distinguish between the lithology of sand and mud (Figure 4). Vp/Vs of sandstone shows low-value characteristics, while those of mudstone and coal seam both show high-value characteristics. Thus, reservoir prediction and fine description of the sand body in this area can be conducted using Vp/Vs.

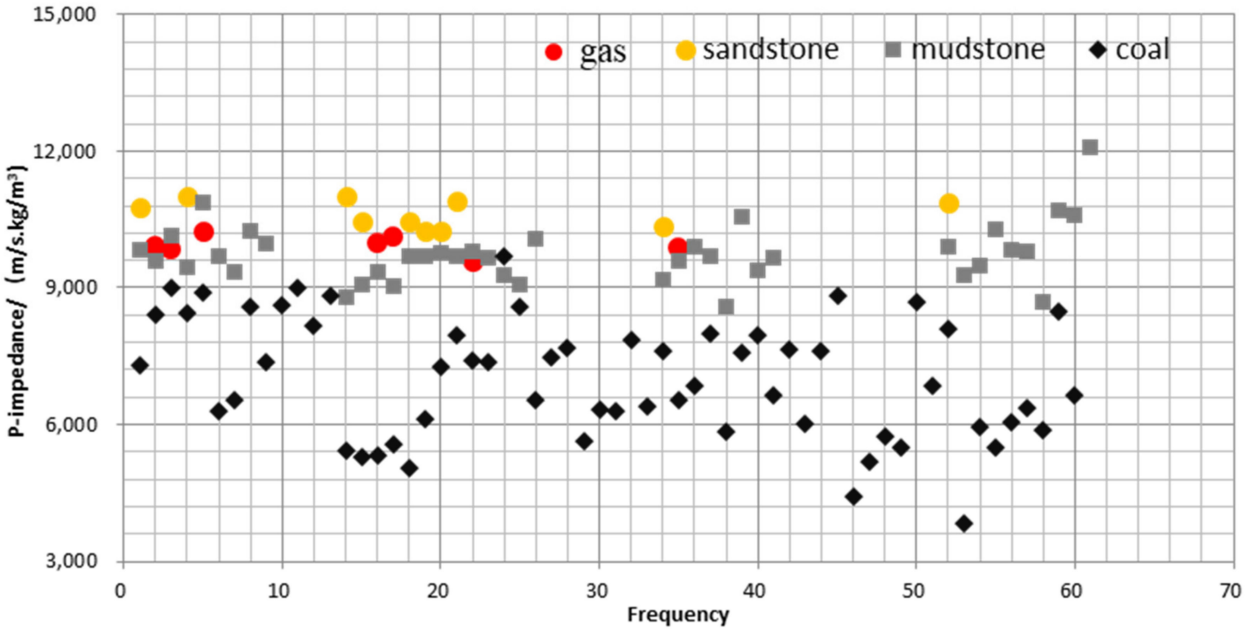

Figure 3. P-impedance distribution characteristics of different lithologies.

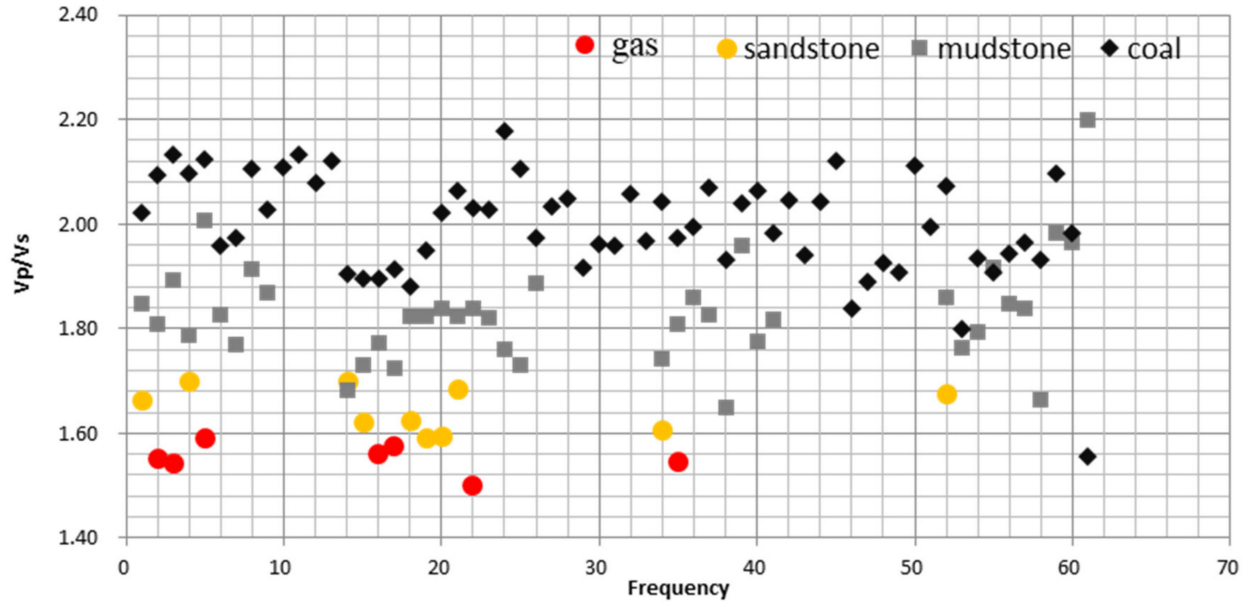

Figure 4. Distribution characteristics of the velocity ratios of compressional and shearing waves for different lithologies.

3.2. Analysis of Factors That Influence Seismic Amplitude

Based on the above petrophysical analysis, the coal seams are characterized by low P-wave impedance and a strong-amplitude trough response in post-stack seismic data. In order to analyze the influence of thin coal seams on the sandstone reservoir, forward models of sand–coal coupling with different numbers of coal seams and seam spacing are designed: the model parameters are shown in Table 1. The seismic forward models of coal seams and sand–coal coupling are compared (Figure 5). Both the coal seams and the gas-bearing sandstone mostly show the characteristics of strong trough bright spots on post-stack seismic data, while a small number shows the characteristics of weak amplitude response due to the influence of coal seam spacing. With the same coal seam spacing, the reflective amplitude of both coal seams and gas-bearing sandstone-top surfaces are stronger the larger the number of coal seams is. With the same number of coal seams, the reflective amplitude of the sandstone-top surfaces gradually increases when the sand–coal spacing decreases. The above analysis suggests that the seismic reflection from the sandstone top is influenced by both the number and spacing of coal seams. It is difficult to analyze the seismic response of sand and coal assemblages on post-stack seismic data because the distribution of coal seams, which is affected by tides, is random in number and spacing.

Table 1. Model parameters of thin gas-bearing sandstone with different AVO types.

Lithology	P Wave Velocity (m/s)	S Wave Velocity (m/s)	Density (g/cm^3)	Vp/Vs
Mudstone	4150	2220	2.63	1.87
Sandstone	4027	2430	2.43	1.65
Coal seam	2700	1350	1.90	2.0

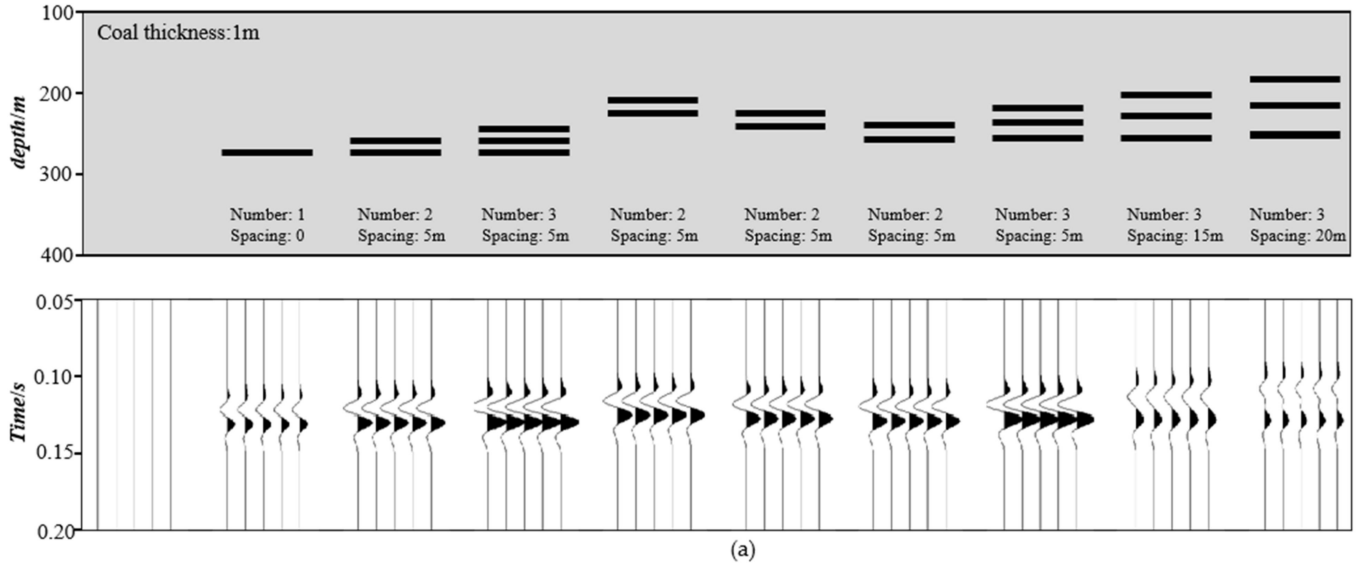

Figure 5. *Cont.*

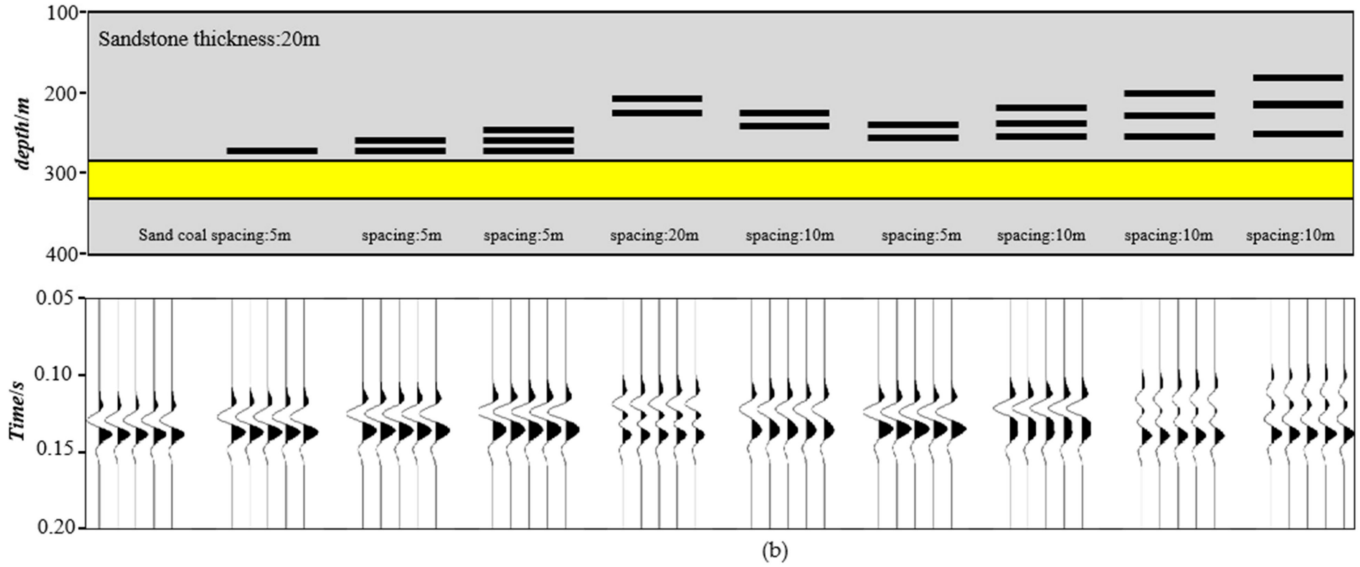

Figure 5. Forward models with coal seams and sand–coal assemblages. (**a**) Geological models with only coal seams; (**b**) geological models with both coal seams and sandstone (without coal seams, the sandstone-top surface shows trough reflection, while the sandstone–coal assemblage may show stronger or weaker amplitude and the response of sandstone cannot be recognized).

3.3. A Method to Suppress Coal Seam Interference Based on Partial Stacked Seismic Analysis

Given that the seismic response characteristics of sandstone–coal assemblages are complex, the response characteristics of coal seams and sandstone cannot be effectively distinguished by conventional seismic data alone, and other means of analysis are required. The statistics for all coal seams and gas-bearing sandstone in the study area (Tables 2 and 3) show that most of the coal seams exhibit low P-impedance, positive gradient and IV AVO type, while gas-bearing sandstone exhibits low P-impedance, negative gradient and II-III AVO type. In the near-gather seismic data, the difference between gas-bearing sandstone and coal seams is not obvious, which is the fundamental reason why their responses cannot be effectively distinguished using only post-stack seismic analysis. However, in the far-gather seismic data, coal seams gradually decrease in energy, while gas-bearing sandstone gradually increases in energy. Thus, the influence of coal seams can be eliminated through the far-gathers of partial post-stack seismic analysis.

Table 2. Statistics concerning elastic parameters and AVO characteristics of drilled coal seams in the Pingbei slope belt.

Lithology	P-Wave Velocity (m/s)	S-Wave Velocity (m/s)	Density (g/cm^3)	Intercept	Gradient	AVO Type
Mudstone	4150	2220	2.63	—	—	—
Coal seam	2700	1350	2.00	−0.3477	0.4657	IV
	2639	1300	2.13	−0.3276	0.4525	IV
	2900	1378	2.10	−0.2894	0.4271	IV
	2698	1290	2.15	−0.3125	0.4504	IV
	2617	1300	2.14	−0.3293	0.4503	IV
	2747	1362	1.90	−0.3646	0.4873	IV
	2956	1605	2.14	−0.2708	0.3237	IV
	2801	1600	2.00	−0.3301	0.3625	IV
	2900	1627	2.02	−0.3085	0.3461	IV
	2760	1529	1.80	−0.3885	0.4535	IV
	2849	1600	2.18	−0.2794	0.3124	IV
	2736	1654	2.07	−0.3245	0.3154	IV
	2619	1344	1.75	−0.4271	0.5417	IV
	2895	1337	1.80	−0.3655	0.5192	IV

Table 3. Statistics concerning elastic parameters and AVO characteristics of drilled sandstone in the Pingbei slope belt.

Lithology	P-Wave Velocity (m/s)	S-Wave Velocity (m/s)	Density (g/cm^3)	Intercept	Gradient	AVO Type
Mudstone	4150	2220	2.63	-	-	-
	4027	2518	2.43	−0.0546	−0.1309	II
	4114	2492	2.42	−0.0459	−0.1004	II
	4300	2402	2.39	−0.0115	−0.0414	II
	4273	2517	2.44	−0.0229	−0.0966	II
	4080	2485	2.47	−0.0399	−0.1148	III
	4361	2743	2.49	−0.0026	−0.2247	III
Sandstone	4136	2492	2.40	−0.0474	−0.0919	II
	4062	2575	2.45	−0.0461	−0.1643	III
	4000	2415	2.41	−0.0621	−0.0708	II
	4230	2473	2.46	−0.0239	−0.0838	II
	4157	2480	2.38	−0.0491	−0.0769	II
	4235	2550	2.42	−0.0314	−0.1151	III
	4070	2515	2.39	−0.0575	−0.1117	III

We simulated pre-stack forward modeling using the wave equation method in the frequency domain because thin coal seam assemblages do not meet the semi-infinite-space hypothesis condition of the Zoeppritz equation. The acoustic wave equation in the time domain can be expressed as

$$\frac{\partial^2 u(x,z,t)}{\partial x^2} + \frac{\partial^2 u(x,z,t)}{\partial z^2} - \frac{1}{v(x,z)^2}\frac{\partial^2 u(x,z,t)}{\partial t^2} = -f(x,z,t) \quad (1)$$

where $v(x,z)$ is the wave velocity in the media, which is a function of position when the media is anisotropic. f is the source function, which is usually set as Ricker wavelet. Take the Fourier transform of t to transform Equation (1) into the frequency domain. $u(x,z,t)$ is transformed into $u(x,z,\omega)$, and $f(x,z,t)$ is transformed into $f(x,z,\omega)$. Therefore, Equation (1) is transformed into

$$\frac{\partial^2 u(x,z,\omega)}{\partial x^2} + \frac{\partial^2 u(x,z,\omega)}{\partial z^2} - \frac{\omega^2}{v^2}u(x,z,\omega) = -f(x,z,\omega) \quad (2)$$

The study area is grided according to a geological model. A finite-difference operator is used to discretize the continuity equation at each grid element. The difference equation is solved, and an approximation of the solution at each grid element is obtained. Surface receivers are designed based on an actual observation system so that the real seismic reflection records can be obtained. Figure 6 shows a comparison of the forward modeling results as obtained by the Zoeppritz equation and the wave equation. The amplitude energy of coalbed-top surface decreases with an offset in the wave equation model, whereas it increases with an offset in the Zoeppritz equation model. These results indicate the wave equation model agrees better with the actual seismic response of coal beds than the Zoeppritz equation model.

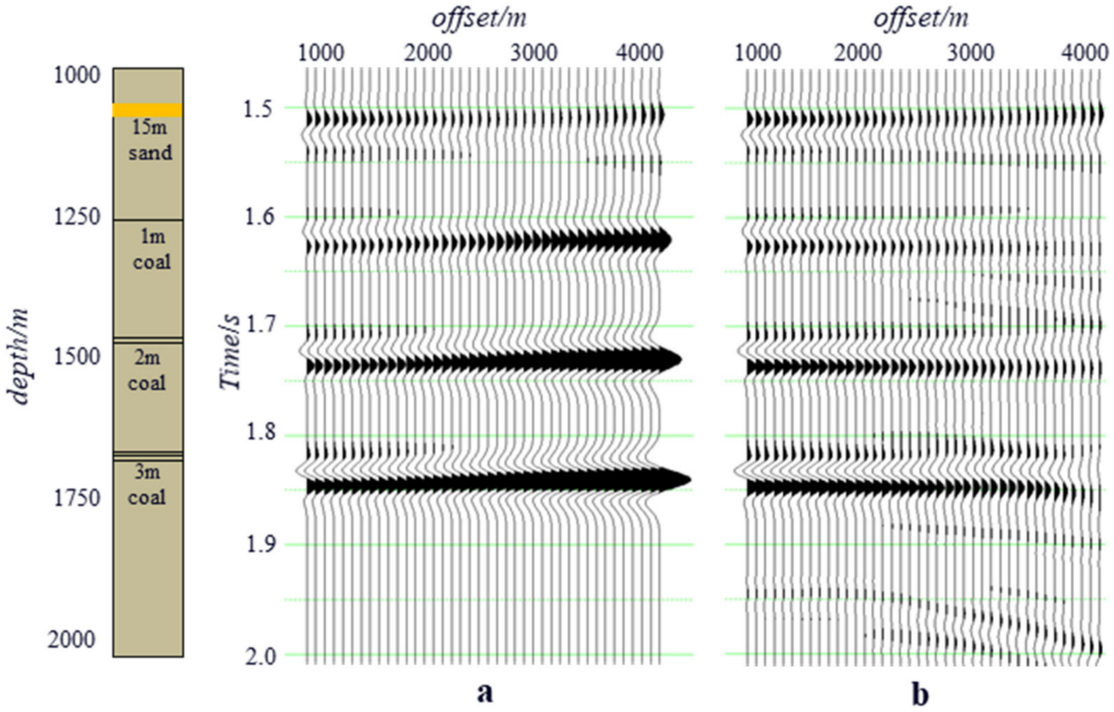

Figure 6. Comparison of the forward modeling results obtained using the Zoeppritz equation and the wave equation. (**a**) Zoeppritz equation modeling result; (**b**) wave equation modeling result.

In order to confirm that the far angle partial stacked seismic data can eliminate the interference of coal seams, forward models with different sand–coal spacing are designed. The parameters of the models are the same as in Table 1, where the thickness of each coal seam is 1 m, and the sand–coal spacing gradually changes from 1 m to 80 m. The finite-difference wave equation forward modeling method, using the aforementioned frequency domain and a Ricker wavelet of 25 Hz, is employed. The partial stacked seismic data with different angles (Figures 7 and 8) show that, in the near-gather stack seismic data, the trough energy of the sandstone top is enhanced by the influence of the coal seam, and the amplitude of the gas-containing sandstone increases by 1.7 times relative to the sandstone without a coal seam. With the increase in the partial stack angle, the influence of the coal seam on the amplitude of the sandstone-top surface becomes weaker and weaker. The amplitude of the sandstone with a coal seam is the same as that of the sandstone without a coal seam in the far-gather seismic data. Based on the above analysis, it is believed that a far-angle partial stacked seismic analysis can better eliminate the influence of the coal seam and improve the accuracy of sandstone prediction.

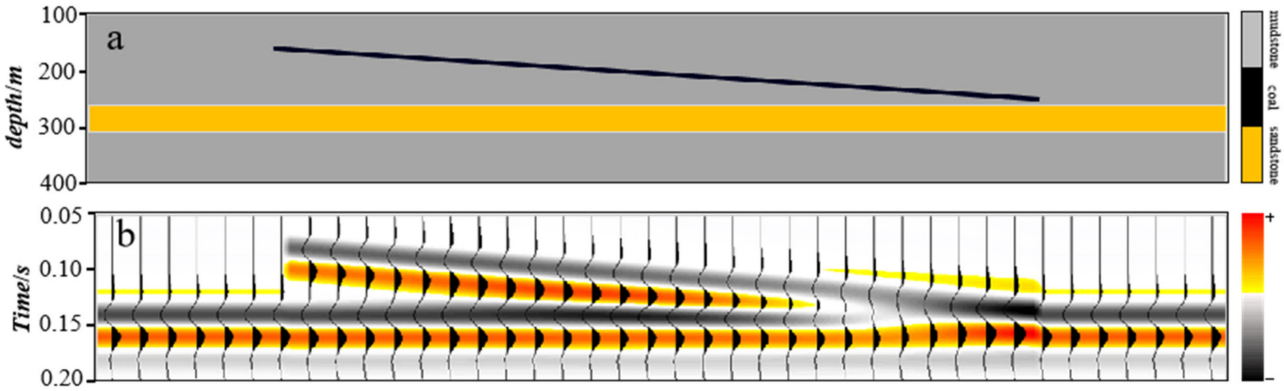

Figure 7. *Cont.*

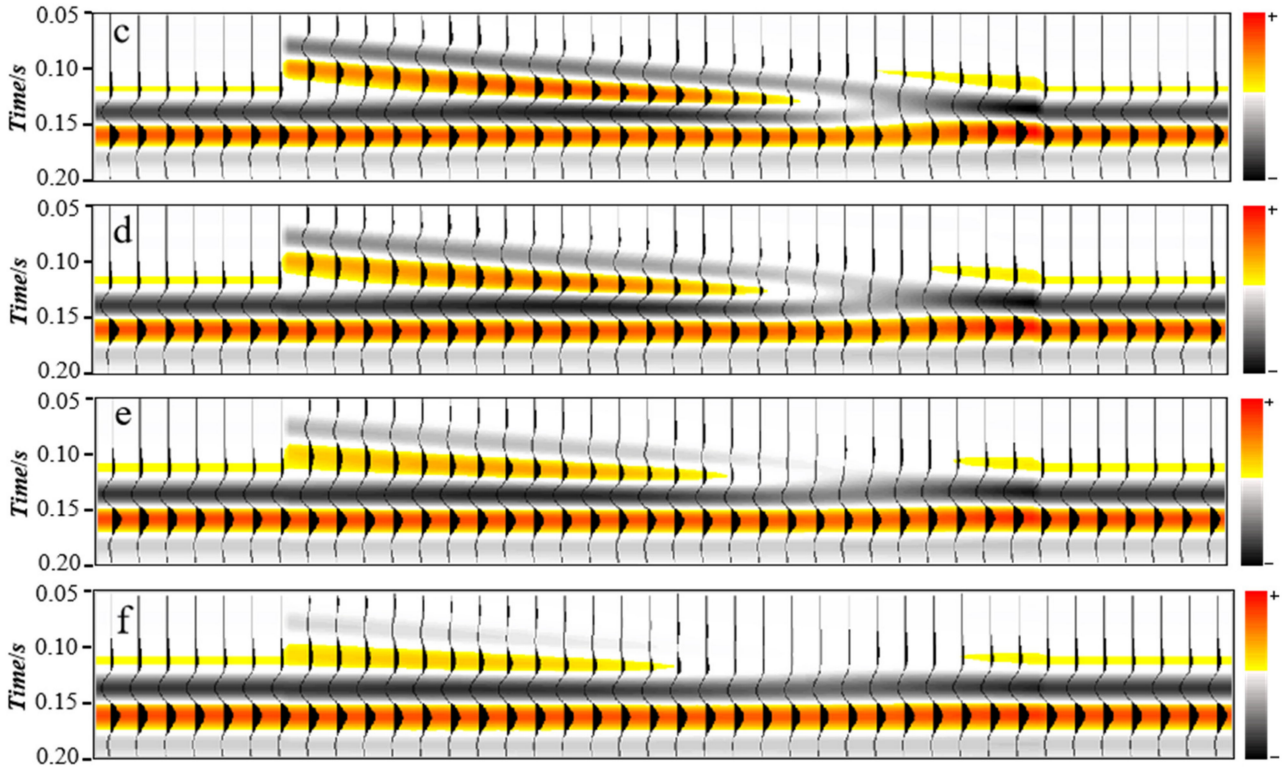

Figure 7. Seismic response of the partial stacked seismic analysis for sandstone–coal assemblage at different stack angles: (**a**) geologic model; (**b**) partial stacked seismic analysis 0–7°; (**c**) partial stacked seismic analysis 7–14°; (**d**) partial stacked seismic analysis 14–21°; (**e**) partial stacked seismic analysis 21–28°; (**f**) partial stacked seismic analysis 28–35°.

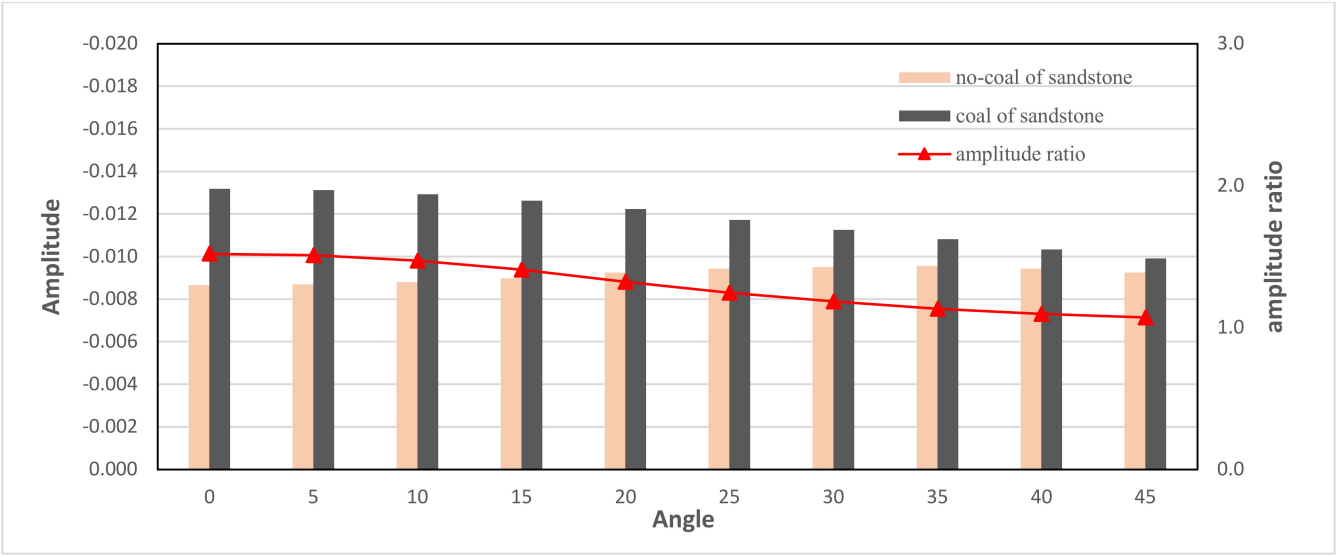

Figure 8. Partial stacked seismic amplitude of sandstone-top surface at different stack angles.

4. Results

Fault-block traps, which are dominated by faults, and structure-lithostratigraphic traps, which are dominated by faults and channel sands, are the main trap types in the study area, so it is important to recognize lithologic boundaries accurately. Sand–coal and mud–coal assemblages have been encountered during the drilling of many wells in the Pinghu Formation. Both the sand–coal and mud–coal assemblages show strong-amplitude bright spot reflections in seismic analyses due to the effect of coal seams. Consider the

seismic profile across Wells X-2 and X-3 as an example (Figure 9a). The P4 layer of Well X-2 is mainly characterized by sand–coal coupling and shows strong-amplitude trough reflection in its seismic profile. The P8 layer of Well X-2 is mainly mud–coal coupling and shows strong-amplitude trough reflection. It is difficult to identify the distribution of sandstone channels in post-stack seismic analysis.

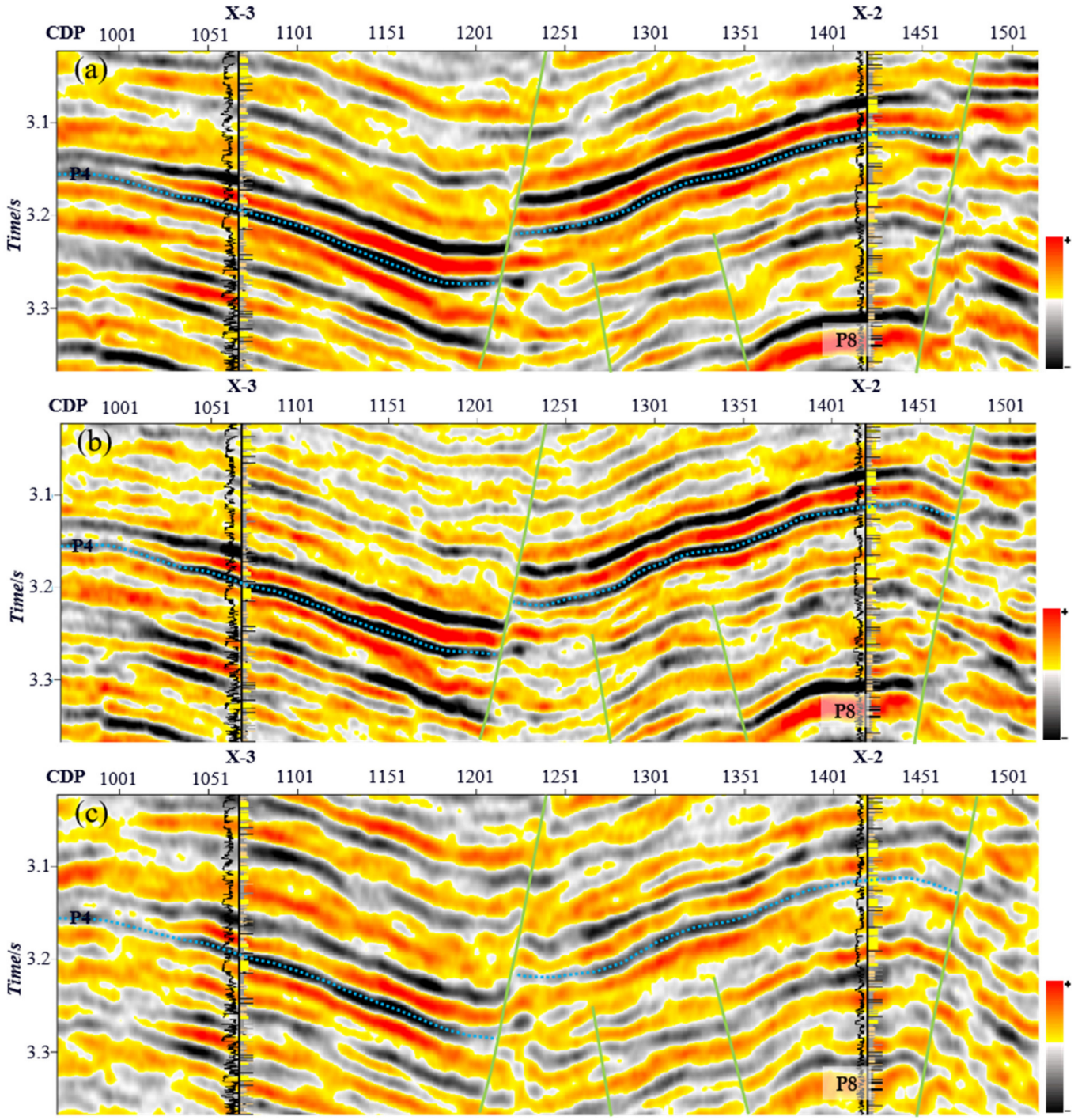

Figure 9. *Cont.*

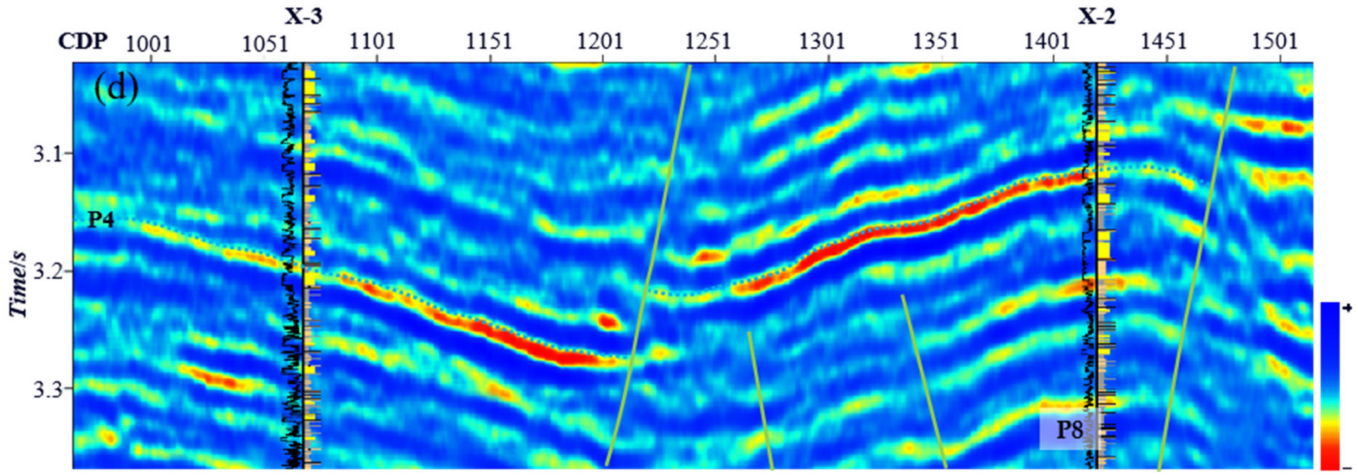

Figure 9. Post-stack and partial stacked seismic profiles across Wells X-2 and X-3. For locations of the profiles, see Figure 1. (**a**) The post-stack seismic profile; (**b**) the near offset partial stacked seismic profile; (**c**) the far-offset partial stacked seismic profile; (**d**) P + G hydrocarbon detection profile.

In order to eliminate the influence of the coal seam, the partial stack seismic profiles at different angles are analyzed (Figure 9b,c). It is found that the coal seam exhibits a very low P-impedance and a strong-amplitude reflection characteristic on the near-gather seismic data, which is a similar result to that of the post-stack seismic data, and is not conducive to a fine characterization of the sandstone. However, in the far-offset partial stack seismic profile, the coal seam shows a class-IV AVO signature with a strong amplitude in the near angle and a weak amplitude in the far angle, so the amplitude of the mudstone–coal stratigraphic assemblage (P8 in Well X-2) is significantly weakened in the far angle gather and in the P + G hydrocarbon detection profile (Figure 9d). In contrast, the sand–coal stratigraphic assemblage (P4 in Well X-2) shows a strong-amplitude reflection signature in the far-offset partial stack seismic profile and exhibits a stream channel in the downward direction of the strong trough. Moreover, gas-containing characteristics can be found in P4 in the P + G hydrocarbon detection profile (Figure 9d). Weak amplitude in the far-offset partial stack seismic analysis should be considered a predictor of a coal seam, while strong amplitude in the far-offset partial stack seismic analysis should be considered a predictor of gas-containing sandstone. The actual drilling result is reliably consistent with the predictions. The sand–coal assemblage can show either a strong or a weak amplitude in the minimum amplitude attribute of the P4 layer due to variation in sand–coal spacing and in the number and thickness of coal seams, and a large number of false bright spot reflections can also be seen (Figure 10a). In the minimum amplitude attribute of the far-offset partial stack seismic analysis, the false bright spot reflections have been effectively eliminated, and the pattern of braided channels is more clearly defined. Thus, it is evident that the far-offset partial stack seismic analysis is of great benefit in advanced reservoir prediction and description.

We evaluated a structure-lithostratigraphic trap and designed Well X-3 in the footwall based on the temporal and spatial relationships between the braided channels and faults. A 22 m thick gas-containing layer with 12.6% porosity in P4 was encountered by Well X-3, and the proven reserve of natural gas in the P4 layer increased by about 1.4 billion cubic meters. Three wells were successfully drilled, and the drilling success rate improved from 50% to 80% thanks to the method introduced in this paper. The far-gather seismic attribute was applied successfully and was proven helpful in the exploration of low-porosity, low-permeability reservoirs in the coal-bearing strata in the study area.

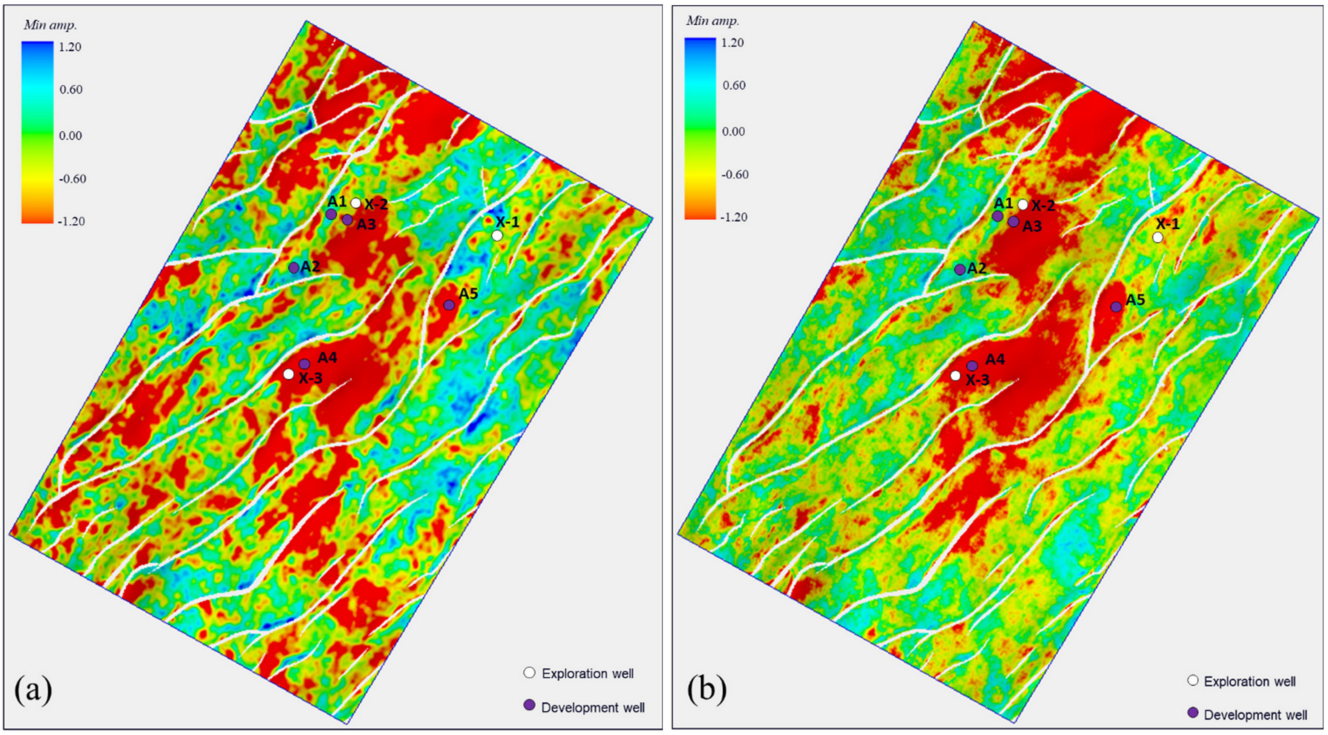

Figure 10. Minimum amplitude attribute of the P4 layer in the study area: (**a**) the minimum amplitude of post-stack seismic analysis; (**b**) the minimum amplitude of far-offset partial stacked seismic analysis.

5. Discussion

Although the interference of coal seams can be effectively reduced by far-offset partial stacked seismic analysis, multi-layer coal seams will cause residual energy illusions in far-gather analysis. In order to exclude the energy abnormality illusion and to demonstrate the applicability of the method described in this paper, we designed a pre-stack forward model of a multi-layer coal seam. The model uses a horizontally layered medium. Three types of strata are simulated: sandstone, a sandstone–coal assemblage (the thicknesses of the three coal seams are 1.0 m, 0.5 m and 1.0 m, and the distance between sandstone and coal is 5 m) and a coal seam (Figure 11).

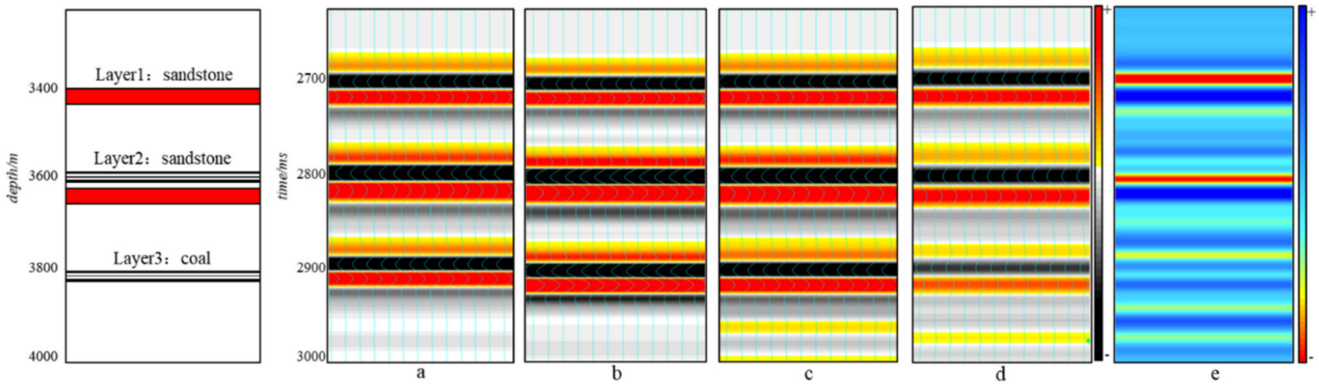

Figure 11. Seismic response of forward models with a sandstone–coal assemblage at different stack angles: (**a**) post-stack seismic analysis; (**b**) partial stacked seismic analysis 1–15°; (**c**) partial stacked seismic analysis 15–30°; (**d**) partial stacked seismic analysis 30–45°; (**e**) P + G hydrocarbon detection profile.

The simulation results are shown in Figure 10. The sandstone model exhibits a class-IIb AVO feature, and the trough energy increases as the offset angle increases. The sandstone–

coal assemblage model exhibits a class-IV AVO feature, and its trough energy and frequency are lower than the sandstone model. The coal seam model exhibits a typical class-IV AVO feature, and the trough energy decreases as the offset angle increases. There is a residual energy illusion in the far-gather of the coal seam model, which disturbs the prediction of sandstone, and the greater the thickness of coal seam, the stronger the interference. We analyzed the P + G attribute to exclude the energy abnormality of the multi-layer coal seam. The coal seam shows high Vp/Vs in the P + G attribute, whereas sandstone shows low Vp/Vs. Therefore, we can suppress the coal-bearing interference and improve the drilling success rate using the far-gather seismic attribute integrated with the P + G attribute.

6. Conclusions

We investigated the seismic response of sandstone–coal assemblages, both by analyzing the petrophysical and AVO characteristics of sandstone and coal seams and by forward modeling sandstone–coal assemblages. A method of suppressing coal seam interference to improve predictions of reservoirs using far-gather seismic attributes has been proposed. Based on these analyses and a successful case study, we draw the following conclusions:

(1) Coal seams are widespread within the Pinghu Formation and have small thicknesses and low impedance characteristics. P-wave impedance can only be used to detect coal seams, whereas Vp/Vs can be used to detect sandstone reservoirs.
(2) The finite-difference acoustic wave equation in the frequency domain can effectively eliminate the interference of the far-offset waveform distortion that is typical of coal seams, and the simulation results are consistent with the actual seismic response characteristics. The forward modeling of sandstone–coal assemblages indicates that the responses of coal seams and sandstone cannot be distinguished by post-stack seismic data, but the interference of coal seams can be eliminated by far-offset partial stacked seismic analysis.
(3) The far-gather seismic attribute has been applied successfully in reservoir prediction and sand body description in the study area, which contributed to the successful exploration of coal-rich strata in the Pingbei slope belt.
(4) The value of popularizing the method introduced in this paper has been proven in both the ECSSB and the Ordos Basin, where the accuracy of reservoir prediction in coal-bearing strata has been improved.

Author Contributions: Methodology, X.Z. and L.D.; software, C.Y.; investigation, Y.M.; data curation, R.Z. and Y.L.; writing—original draft preparation, Y.M.; writing—review and editing, X.W.; visualization, M.L. All authors have read and agreed to the published version of the manuscript.

Funding: This research received no external funding.

Institutional Review Board Statement: Not applicable.

Informed Consent Statement: Not applicable.

Data Availability Statement: Data available from the authors upon request.

Conflicts of Interest: The authors declare no conflict of interest.

References

1. Abbas, A.; Zhu, H.T.; Zeng, Z.W.; Zhou, X.H. Sedimentary facies analysis using sequence stratigraphy and seismic sedimentology in the Paleogene Pinghu Formation, Xihu Depression, East China Sea Shelf Basin. *Mar. Pet. Geol.* **2018**, *93*, 289–297. [CrossRef]
2. Lei, C.; Yin, S.Y.; Ye, J.R.; Wu, J.F. Geochemical Characteristics and Hydrocarbon Generation History of Paleocene Source Rocks in Jiaojiang Sag, East China Sea Basin. *Editor. Comm. Earth Sci. J. China Univ. Geosci.* **2021**, *46*, 3575–3587.
3. Liu, J.S.; Zhang, S.P. Natural gas migration and accumulation patterns in the central-north Xihu Sag, East China Sea Basin. *Nat. Gas Geosci.* **2021**, *32*, 1163–1176.
4. Liu, J.S.; Li, S.X.; Qin, L.Z.; Yi, Q.; Chen, X.D.; Kang, S.L.; Shen, W.C.; Shao, L.Y. Hydrocarbon generation kinetics of Paleogene coal in Xuhu sag, East China Sea Basin. *Acta Pet. Sin.* **2020**, *41*, 1174–1187.
5. Su, A.; Chen, H.H.; Wu, Y.; Lei, M.Z.; Li, Q.; Wang, C.W. Genesis, origin and migration-accumulation of low-permeable and nearly tight-tight sandstone gas in the central western part of Xihu sag, East China Sea Basin. *Acta Pet. Sin.* **2018**, *92*, 184–196.

6. Diessel, C.F. *Coal-Bearing Depositional Systems*; Springer: Berlin/Heidelberg, Germany, 1992.
7. Zou, F.; Xue, Y.J. Strong amplitude suppression of coal seam based on synchrosqueezed wavelet transform. *Prog. Geophys.* **2018**, *33*, 1198–1204.
8. Liu, L.; Zhang, Q.; Zhang, J.H.; Ban, L.; Li, J.L. Application of the Strong Shielding Peeling Technique Based on Matching Pursuit Algorithm in the Reservoir Prediction of Fan 159 Well Block. *Comput. Tomogr. Theory Appl.* **2016**, *25*, 331–337.
9. Liu, J.; Zhang, Z.T.; Liu, D.L. Sediment boundary identification and fluid detection for the seismic data with strong background reflections. *Geophys. Prospect. Pet.* **2016**, *55*, 142–149.
10. Han, W.G.; Zhang, J.G. Theoretical study on characteristic of weak signal and its identification. *Oil Geophys. Prospect.* **2011**, *46*, 232–236.
11. Ping, A. Application of Multi-Wavelet Seismic Trace Decomposition and Reconstruction to Seismic Data Interpretation and Reservoir Characterization. In Proceedings of the SEG/New Orleans Annual Meeting. 2006. Available online: https://onepetro.org/SEGAM/proceedings-abstract/SEG06/All-SEG06/SEG-2006-0973/93194?redirectedFrom=PDF (accessed on 10 January 2022).
12. Ping, A. Case Studies on Stratigraphic Interpretation and Sand Mapping Using Volume-Based Seismic Waveform Decomposition. In Proceedings of the SEG/New Orleans Annual Meeting. 2006. Available online: https://library.seg.org/doi/10.1190/1.2370307 (accessed on 10 January 2022).
13. Wang, X.X.; Yu, S.; Li, S.; Zhang, N.D. Two parameter optimization methods of multi-point geostatistics. *J. Petrol. Sci. Eng.* **2022**, *208*, 109724. [CrossRef]
14. Zhang, Y.Y.; Wei, X.W.; Tan, M.Y.; Gao, Q.J.; Zhu, D.R.; Li, S.X. Removal of seismic strong shield interface based on compressed sensing technology and its application. *Lithol. Reserv.* **2019**, *31*, 85–91.
15. Gu, W.; Zhang, X.; Xu, M.; Liang, H.; Zhang, D.J.; Luo, J.; Zheng, H. High precision prediction of thin reservoir under strong shielding effect and its application: A case study from Sanzhao Depression, Songliao Basin. *Geophys. Prospect. Pet.* **2017**, *56*, 439–448.
16. Wan, L.; Hurter, S.; Bianchi, V.; Li, P.; Wang, J.; Salles, T. The roles and seismic expressions of turbidites and mass transport deposits using stratigraphic forward modeling and seismic forward modeling. *J. Asian Earth Sci.* **2022**, *229*, 105110. [CrossRef]
17. Tomassi, A.; Trippetta, F.; Franco, R.; Ruggieri, R. From petrophysical properties to forward-seismic modeling of facies heterogeneity in the carbonate realm (Majella Massif, central Italy). *J. Pet. Sci. Eng.* **2022**, *211*, 110242. [CrossRef]
18. Wang, X.X.; Hou, J.G.; Li, S.H.; Dou, L.X.; Song, S.H.; Kang, Q.Q.; Wang, D.M. Insight into the nanoscale pore structure of organic-rich shales in the Bakken Formation, USA. *J. Pet. Sci. Eng.* **2019**, *176*, 312–320. [CrossRef]
19. Juan, C.M.; Ghisays, A.; Montes, L. AVO analysis with partial stacking to detect gas anomalies in the GÜEPAJÉ-3D project. *Geofís. Int.* **2013**, *52*, 249–260.
20. Ismail, A.; Ewida, H.F.; Al-Ibiary, M.G.; Zollo, A. Application of AVO attributes for gas channels identification, West offshore Nile Delta, Egypt. *Pet. Res.* **2020**, *5*, 112–123. [CrossRef]
21. Farfour, M.; Foster, D. New AVO expression and attribute based on scaled Poisson reflectivity. *J. Appl. Geophys.* **2021**, *185*, 104255. [CrossRef]
22. Yi, B.Y.; Lee, G.H.; Horozal, S. Qualitative assessment of gas hydrate and gas concentrations from the AVO characteristics of the BSR in the Ulleung Basin, East Sea (Japan Sea). *Mar. Pet. Geol.* **2011**, *28*, 1953–1966. [CrossRef]
23. Wang, X.C.; Pan, D.Y. Application of AVO attribute inversion technology to gas hydrate identification in the Shenhu Area, South China Sea. *Mar. Pet. Geol.* **2017**, *80*, 23–31. [CrossRef]
24. Liu, L.; Liu, L.H.; Wo, Y.J.; Sun, W. Pre-stack elastic parameter inversion of ray parameters. *J. Appl. Geophys.* **2019**, *162*, 13–21. [CrossRef]
25. Jiang, X.D.; Cao, J.X.; Hu, J.T. Pre-stack gather optimization technology based on an improved bidimensional empirical mode decomposition method. *J. Appl. Geophys.* **2020**, *177*, 104026.
26. Li, C.Y.; Wei, L.; Diao, H.; Cheng, X.; Hou, D.J. Hydrocarbon source and charging characteristics of the Pinghu Formation in the Kongqueting Structure, Xihu Depression. *Pet. Sci. Bull.* **2021**, *6*, 196–208.
27. Li, J.W.; Jiang, B.; Qu, Z.H.; Yin, S.; Xu, J.; Li, P. Tectonic evolution and control of coal in Donghai Xihu Sag. *Coal Geol. Explor.* **2016**, *44*, 22–27.
28. Ding, F.; Liu, J.S.; Jiang, Y.M.; Zhao, H.; Yu, Z.K. Source and migration direction of oil and gas in Kongqueting area, Xihu Sag, East China Sea Shelf Basin. *Mar. Geol. Quat. Geol.* **2021**, *41*, 156–165.
29. Li, J.J.; Jiang, Y.M.; Hou, G.W.; Xie, J.J.; Jiang, X. Constraints of slope break belt on oil and gas trapping-An example from the Pinghu Formation in the Kongqueting area of Pinghu Slope. *Mar. Geol. Quat. Geol.* **2021**, *41*, 141–150.
30. Zhou, X.H.; Gao, S.L.; Gao, W.Z.; Li, N. Formation and distribution of marine-continental transitional lithologic reservoirs in Pingbei slope belt, Xihu sag, East China Sea Shelf Basin. *China Pet. Explor.* **2019**, *24*, 153–164.